

# Radiation Hardening of Ni-Ti Alloy Under Implantation of Inert Gases Heavy Ions

V Poltavtseva<sup>1</sup>, A Larionov<sup>1</sup>, D Satpaev<sup>1</sup> and M Gyngazova<sup>2</sup>

<sup>1</sup>Institute of Nuclear Physics, Almaty, Republic of Kazakhstan

<sup>2</sup>National Research Tomsk Polytechnic University, Tomsk, Russia

E-mail: [poltavtseva@inp.rk](mailto:poltavtseva@inp.rk)

**Abstract.** The consistent patterns of changes in nano- and micro-hardness of Ni-Ti alloy with the shape memory effect after implantation of  $^{40}\text{Ar}^{8+}$  and  $^{84}\text{Kr}^{15+}$  ions depending on phase composition and implantation parameters have been experimentally studied. It has been shown that softening by 4 and 14% near the surface of the two-phase Ni-Ti alloy after implantation of  $^{40}\text{Ar}^{8+}$  and  $^{84}\text{Kr}^{15+}$  ions is connected with the differences in the nanostructure. Hardening of the near-surface layer of this alloy maximum by 118% at  $h = \sim 3 \mu\text{m}$  and single-phase alloy in the entire region of the  $^{40}\text{Ar}^{8+}$  and  $^{84}\text{Kr}^{15+}$  ions range and in the out-range ( $h > R_p$ ) area have been detected. The role of the current intensity of the ions beam in the change of nanohardness for the two-phase Ni-Ti alloy has been established.

## 1. Introduction

The problem of applying ion implantation and/or various beam technologies to produce the hardened coatings with the improved corrosion properties, biochemical compatibility with living tissues of the body and low toxicity for the titanium nickelide based alloys for medical application has not yet been solved. This is associated with the behavior of the dispersion processes, phase transformations, and the features of defect structure and the effect of the phase composition of the titanium nickelide based alloys and implantation parameters. In [1, 2] it was shown that as a result of implantation of MeV-energy gas elements heavy ions at relatively the same parameters the dispersion degree of the two-phase alloy surface decreases with the increase of the ion mass accompanied by the radiation-induced phase transformation B19'→B2, formation of the fine-dispersed or track structure, the two-layered radiation-hardened near-subsurface structure. The effect of  $E_{\text{ion}}$ , M, Z, J parameters on tracks evolution in two-phase and single-phase Ni-Ti alloy [2] and the effect of ion charge on the hardening of the surface layer [3] were established. The provided results suggest new possibilities of modification by implantation of inert gases heavy ions of the titanium nickelide based alloys. However, it is required to perform a comprehensive and thorough study of their structure, physical and mechanical properties, the characteristics of phase transformations, hardening/softening and etc.

The aim of the present investigations is to study the characteristics of changes in nano - and micro-hardness in the modified layer of Ni-Ti alloy after implantation of argon and krypton heavy ions of MeV energy depending on phase composition and implantation parameters.

## 2. Experimental methods and material

We studied the Ni-Ti commercial alloy with Ni of 53.46 wt.% and Ti of 46.54 wt.%, preferably consisting of NiTi with the B2 structure (austenite), NiTi with B19 structure (martensite) and a minor content of Ti, excess Ni in the form of solid solution and process particles similar in composition to  $\text{Ti}_2\text{Ni}(\text{C})$  [1]. Before implantation, a proven technology was used to prepare the surface of the samples: cutting out by the method of spark cutting followed by wet mechanical polishing and buffing with GOI paste. The sample quality was evaluated by the methods of optical metallography and scanning electron microscopy. Based on certification by the method of X-ray structural analysis we have selected the samples of Ni-Ti alloy with the titanium nikelid phase ratio B19'/B2 equal to 0.6-0.7 (two-phase alloy)



for investigations. The single-phase alloy with the B2 structure (austenite) was produced by annealing of two-phase samples in the vacuum ( $\sim 10^{-4}$  Pa) oven for 1 h at 510 K.

Implantation of  ${}_{40}\text{Ar}^{8+}$  ions (70 MeV, 100 and 80 nA/cm<sup>2</sup>) and  ${}_{84}\text{Kr}^{15+}$  (147 MeV, 94, 70 and 30 nA/cm<sup>2</sup>) was performed with DC-60 cyclotron of the Eurasian University (Astana) under comparable parameters  $A/Z = \sim 5$ ,  $E_{\text{ion}} = 1.75$  MeV/nucl,  $\Phi t = 1 \times 10^{19}$  ion/m<sup>2</sup>. The area of radiation treatment was  $\sim 1 \times 10^{-4}$  m<sup>2</sup>. The samples temperature in the process of irradiation was below 370 K.

Measurements of nano – and microhardness of the Ni-Ti alloy samples were performed by the method of sclerometry [2, 3] and by Vickers' method depending on the applied load in the range of  $1 \pm 200$  mN and  $0.098 \pm 4.9$  N using the nanohardness gage «NanoScan-Compact» and microhardness gage «PMT-3M» (Russia) respectively. The accuracy was 1% for nanohardness measurement and 3-4% for microhardness measurement. The thickness of surface and near-surface layers at each applied load was determined by the depth of scratches and impressions. The surface roughness was evaluated according to the scanned images.

### 3. Experimental results and discussion

The results of nanohardness measurement depending on surface layer thickness for two-phase and single-phase Ni-Ti alloys before and after implantation of  ${}_{40}\text{Ar}^{8+}$  and  ${}_{84}\text{Kr}^{15+}$  ions are represented in Fig. 1. It is shown that the values of surface nanohardness for these alloys differ in 1.8 times, caused mainly by the difference in hardness of martensite and austenite.

In the case of two-phase alloy the character  $H(h)$  of the curves is similar, with the maximum near the surface (Fig. 1a). The highest value of nanohardness is observed for un-implanted two-phase Ni-Ti alloy (Fig. 1a, curve 1). The paper [1] shows that it is connected with formation of  $\text{Ni}_3\text{Ti}_3\text{O}$  compound in the deformation-hardened layer in the process of Ni-Ti alloy samples preparation.

The implantation of  ${}_{40}\text{Ar}^{8+}$  and  ${}_{84}\text{Kr}^{15+}$  ions results in softening of the surface layer by 4 and 14% near the surface respectively and slightly in the layer of  $>120$  nm thickness (curves 2 and 3), compared to un-implanted two-phase alloy (Fig. 1a, curve 1). Softening of the modified surface layer of two-phase alloy, regardless of the ion mass, can be caused by sputtering of the deformation-hardened layer, as indicated by the shift of maxima on  $H(h)$  - curves to the modified surface, by decreasing of martensite due to radiation-stimulated phase transformation  $\text{B19}' \rightarrow \text{B2}$  [1, 4] and the change in the surface microstructure [1, 5].

According to X-ray diffraction analysis data [1] the process of  ${}_{40}\text{Ar}^{8+}$  and  ${}_{84}\text{Kr}^{15+}$  ions implantation is characterized by the radiation stimulated transformation  $\text{B19}' \rightarrow \text{B2}$  occurring in the surface layer. The phase composition of the surface consists essentially of the phase with the structure B2 (austenite). However, the degree of dispersion and change of the surface structure, as established in [1, 5], depends on the mass of heavy ions under comparable parameters of implantation. Indeed, in [1] based on the studies data obtained by scanning electron microscopy and X-ray spectral analysis it was shown that for the two-phase alloy, firstly, the degree of dispersion decreases and the role of surface ion polishing increases with the ion mass growth. This conclusion is also supported by the difference in the values of maxima shift (Figure 1a, curves 2 and 3).

Secondly, the interaction of  ${}_{40}\text{Ar}^{8+}$  and  ${}_{84}\text{Kr}^{15+}$  ions with the surface of two-phase alloy is accompanied by formation of uniform fine-dispersed (up to 1 nm) structure and inhomogeneous larger (up to 25 nm) track structure respectively [5]. From comparison of the above mentioned causes of the surface layer softening of the two-phase alloy, it can be concluded that the difference in the nanostructure is one of the main reasons for the differences in nanohardness after implantation of  ${}_{40}\text{Ar}^{8+}$  and  ${}_{84}\text{Kr}^{15+}$  ions.

In contrast to the two-phase alloy (Figure 1 a), the single-phase alloy is characterized by hardening near the surface and in the layer  $\geq 50$  nm thick by 8.6 and 64%, respectively as the result of implantation of  ${}_{84}\text{Kr}^{15+}$  ions (figure 1b, curve 3). However, in case of  ${}_{40}\text{Ar}^{8+}$  ions implantation hardening by 66% in average is observed only in the layer  $\geq 75$  nm thick, and there is no maximum on  $H(h)$  - curve (Figure 1b, curve 2). The data obtained for the single-phase alloy also support the conclusion about the influence of ion mass on the degree of surface dispersion.

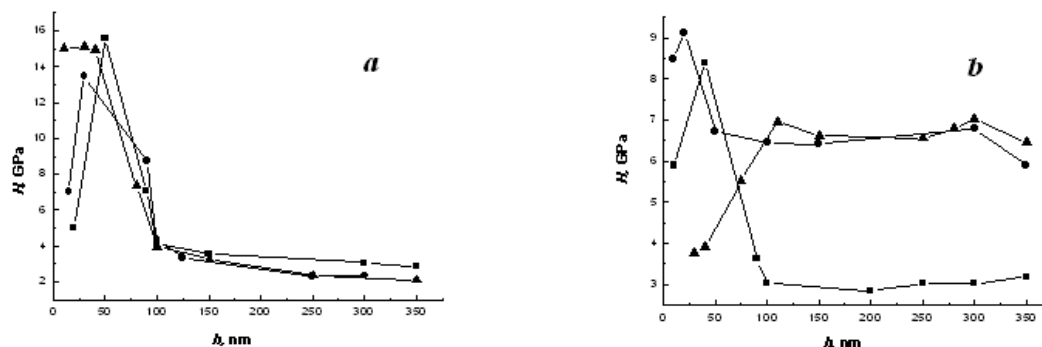


**Figure 1.** Dependence of nanohardness for two-phase (a) and single-phase Ni-Ti alloy (b) before (curve 1) and after implantation of  $^{40}\text{Ar}^{8+}$  (curve 2) and  $^{84}\text{Kr}^{15+}$  (curve 3) ions on thickness of surface layer

It follows from the analysis of the arithmetic mean values of roughness height obtained by measuring of the roughness curves, that the surface quality is practically independent from the phase composition during implantation of  $^{84}\text{Kr}^{15}$  ions. However, as the result of implantation of  $^{40}\text{Ar}^{8+}$  ions, the surface roughness of the two-phase alloy, on the contrary, is 1.6 times higher than for the single-phase alloy, whereas this ratio is 1.9 times for the unimplanted alloys. Thus, the marked roughness data also indicate the predominant role of the ion polishing process during implantation of heavier krypton ions, and dispersion during interaction of lighter argon ions with the surface of Ni-Ti alloy.

The patterns of microhardness changes depending on thickness of the near-surface layer for two-phase and single-phase Ni-Ti alloys before and after implantation of  $^{40}\text{Ar}^{8+}$  и  $^{84}\text{Kr}^{15+}$  ions are shown in Figure 2. Similar to nanohardness (Figure 1), firstly, the microhardness values of the near-surface layer of these alloys vary, but in a less (1.3-time) degree.

Secondly,  $H_n(h)$  - curves are similar for two-phase alloy (Figure 2a) and different for single-phase alloy (Figure 2b) after implantation of heavy ions of inert gases. This measured  $H_n(h)$  - curve of single-phase alloy after implantation of  $^{40}\text{Ar}^{8+}$  ions (Figure 2b, curve 2) is similar to the corresponding curves for two-phase alloy (Figure 2a, curves 2 and 3), and after implantation of  $^{84}\text{Kr}^{15+}$  ions it is more flat (Figure 2b, curve 3). Thirdly, the unimplanted two-phase alloy softens with increasing thickness of the near-surface layer (Figure 2a, curve 1), whereas in case of single-phase alloy, on the contrary, strengthening is occurring (Figure 2b, curve 1).

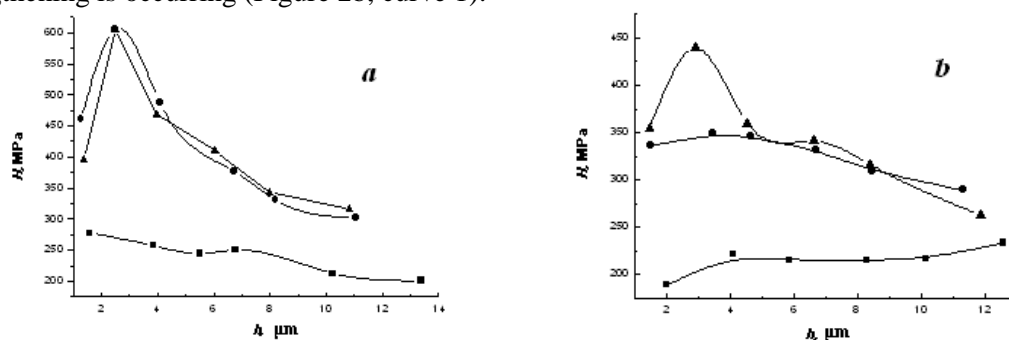


**Figure 2.** Dependence of microhardness for two-phase (a) and single-phase Ni-Ti alloy (b) before (curve 1) and after implantation of  $^{40}\text{Ar}^{8+}$  (curve 2) and  $^{84}\text{Kr}^{15+}$  (curve 3) ions on thickness of near-surface layer

We shall note that, in contrast to the surface layer (Figure 1) the radiation hardening of Ti-Ni alloy (Figure 2) is occurring for the near-surface layer, irrespective of phase composition and ion mass. The maximum degree of hardening is observed  $\sim 3 \mu\text{m}$  deep and it equals to 118% for two-phase alloy ( $^{40}\text{Ar}^{8+}$ ,  $^{84}\text{Kr}^{15+}$ ) and 99 ( $^{40}\text{Ar}^{8+}$ ) and 58% ( $^{84}\text{Kr}^{15+}$ ) for single-phase alloy. These data confirm the

formation of two-layered structure of the near-surface layer with various degree of hardening [1]. Besides, the hardening of the near-surface layer is observed for both alloys in thicknesses greater than the projected range of  $R_p$  ions in Ni-Ti alloy ( $R_p = 8.6$  and  $10.1 \mu\text{m}$  respectively for  ${}_{40}\text{Ar}^{8+}$  and  ${}_{84}\text{Kr}^{15+}$  ions), i.e. in the out-range area.

The comparison of the implantation parameters shows that the current intensity for  ${}_{40}\text{Ar}^{8+}$  ( $80 \text{ nA/cm}^2$ ) and  ${}_{84}\text{Kr}^{15+}$  ( $30 \text{ nA/cm}^2$ ) ions beam in the case of single-phase alloy is lower than for  ${}_{40}\text{Ar}^{8+}$  ( $100 \text{ nA/cm}^2$ ) and  ${}_{84}\text{Kr}^{15+}$  ( $94 \text{ nA/cm}^2$ ) ions during implantation of two-phase alloy. In [5] it was found that the current intensity of  ${}_{84}\text{Kr}^{15+}$  ions beam has a significant impact on the microstructure of two-phase Ni-Ti alloy surface. In this regard, the measurements of nano - and micro-hardness of two-phase alloy after implantation of  ${}_{84}\text{Kr}^{15+}$  ions were performed with varying of the beam current intensity. The obtained results are shown in Figure 3.

As it can be seen in Figure 3a, the character of  $H(h)$  - curves in the layers (up to  $100 \text{ nm}$  thick) is the same for all values of intensity. The maximum value of nanohardness is observed in case of  $J = 70 \text{ nA/cm}^2$  (curve 2). A decrease in nanohardness by 24% during implantation of ions with the maximum ( $94 \text{ nA/cm}^2$ ) intensity (curve 3) may be associated with a high degree of dispersion processes [1, 4] and with the presence of tracks formations in the surface microstructure [4] compared to the intensity of  $70 \text{ nA/cm}^2$ .

The minimum value of nanohardness in the layer up to  $50 \text{ nm}$  thick (curve 1) is observed at minimum ( $23 \text{ nA/cm}^2$ ) intensity and caused mainly by predominance of smaller tracks in the near-surface layer microstructure [4]. However, in the  $> 120 \text{ nm}$  thick layer (Figure 3),  $H(h)$  curve after ions implantation with the minimum intensity, in contrary, is higher than for the case with the maximum intensity.

In case of microhardness the character of  $H_\mu(h)$  - curves in the layer of  $< 5 \text{ microns}$ , is the same for all values of the beam current intensity (Figure 3b). However, the maximum value of microhardness corresponds to the maximum intensity (curve 3), and its value is practically the same (curves 1 and 2) for lower intensities. And the intensity value has no evident impact on the microhardness value in the out-range area where radiation hardening of two-phase and single-phase alloys (Figure 2a) are detected.

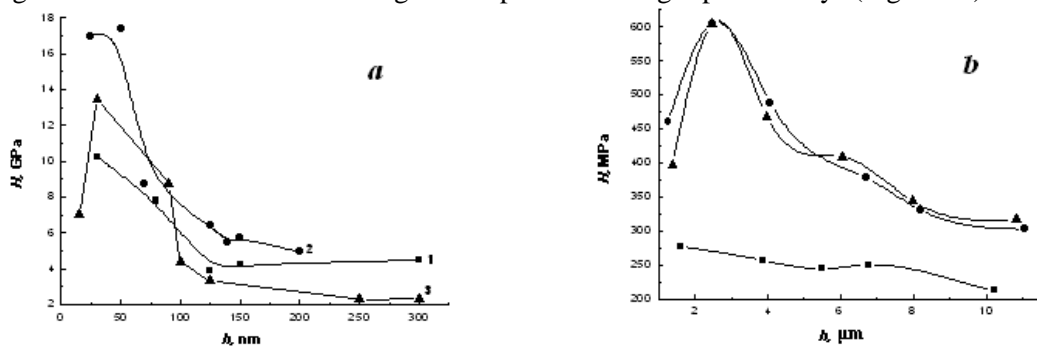


**Figure 3.** Change of nano – and microhardness of two-phase Ni-Ti alloy from intensity of  ${}_{84}\text{Kr}^{15+}$  ions beam current: 1 – 23; 2 – 70; 3 –  $94 \text{ nA/cm}^2$

The paper [3] also specified the role of  ${}_{84}\text{Kr}$  ions charge in the nanohardness change depending on thickness of the surface layer of two-phase Ni-Ti alloy. It was found that near the surface the nanohardness value increases in 2.6 times with the decrease of the ions charge from  $15+$  to  $11+$  and equalizes in  $800 \text{ nm}$  thick layers. The increase of  ${}_{84}\text{Kr}$  ions charge, as shown in [5], occurs with the slight increase in the number of individual tracks.

#### 4. Conclusion

Thus, the study shows that softening by 4 and 14% near the surface of two-phase Ni-Ti alloy after implantation  ${}_{40}\text{Ar}^{8+}$  и  ${}_{84}\text{Kr}^{15+}$  ions at relatively same parameters of  $A/Z$ ,  $E/\text{nucleon}$ ,  $\Phi t$ ,  $J$  is mainly caused by formation of fine-dispersed and track structure, respectively. The near-surface layer of this alloy, on the contrary, hardens regardless of the ion type, maximum by 118% at the depth  $\sim 3 \mu\text{m}$ . It is

found that in the case of single phase Ni-Ti alloy hardening is observed in the entire region of heavy ion range, except the area near the surface due dispersion of the deformation-hardened layer by  ${}_{40}\text{Ar}^{8+}$  ions. The hardening of both alloys in the out-range area ( $h > R_p$ ) is also observed. It is shown that the effect of the current intensity of the  ${}_{84}\text{Kr}^{15+}$  ions beam on the nanohardness value in the case of two-phase Ni-Ti alloy is associated with the change of the track structure.

### Acknowledgements

This work was partially supported by The Ministry of Energy of the Republic of Kazakhstan within the framework of the budget program “Applied scientific research of technological character” and by The Ministry of Education and Science of the Russian Federation in part of the science activity program.

### References

- [1] Poltavtseva V, Kislitsin S and Satpaev D 2015 *IOP Conf. Series: Materials Science and Engineering*, **81** 01234
- [2] Poltavtseva V 2015 *Proc. XI Int. Conf. on Interaction of Radiation with Solids (Minsk)* (Publishing House Center BSU) p 141
- [3] Larionov A, Poltavtseva V and Kislitsin S 2015 *Proc. XII Int. Conf. on Advanced technologies, equipment and analytical systems for materials and nano-materials (Yst-Kamenogorsk)* (Publishing House Center VKGTU) p 283
- [4] Gogolinskiy K, Lvova N and Useinov A 2007 *Plant laboratory* **73** p 28
- [5] Poltavtseva V, Kislitsin S, Koval N and Oskomov K 2012 *Izv. Vyssh. Uchebn. Zaved. Fiz.* **12/3** p 41